EFFECT OF NONLINEAR EXTERNAL CIRCUIT ON ELECTROSTATIC DAMPING FORCE OF MICRO ELECTRET GENERATOR

Daigo Miki, Yuji Suzuki, and Nobuhide Kasagi
Dept. of Mechanical Engineering, the University of Tokyo, Tokyo, Japan

ABSTRACT

A complete electromechanical model of vibration-driven micro electret power generators has been developed, and its characteristics are directly compared with experimental data to verify the model. Nonlinear power management circuit for rectification and impedance conversion is also assumed. It is found that the electrostatic damping force acting on the seismic mass is dependent on the external circuit. From coupling simulation with a mechanical vibration model, it is also found that the circuit parameters should be optimized dependent on the oscillation condition.

KEYWORDS

Energy harvesting, Electret, Nonlinear circuit, Impedance conversion, Damping force

INTRODUCTION

Energy harvesting using environmental vibration has large potential to replace button batteries used for low power applications such as RFIDs and automotive sensors [1, 2]. Since the frequency range of vibration existing in the environment is below 100 Hz, electret power generators [3-6] should have higher performance than electro- magnetic counterparts.

We recently developed a new high-performance electret material based on amorphous perfluorinated polymer CYTOP, and demonstrated up to 0.7 mW power generation at an oscillation frequency as low as 20 Hz with 1.2 mm_{p-p} amplitude [7]. Edamoto et al. [8] has developed a prototype of CYTOP-electret MEMS generator with parylene springs [9] and a low-power-consumption power managing circuit. Tsutsumino et al. [10] and Marboutin et al. [11] extend the numerical approach of Tada [12] and developed a numerical model of electret generators including parasitic capacitance.

In the present study, we develop a numerical model of the electret generator with a power management circuit, and investigate the effect of nonlinear external circuits on the electrostatic damping force. In addition, we simultaneously solve the equation of mechanical vibration and examine electro/mechanical performance of generators, which is crucial to the optimal design.

POWER GENERATION EXPERIMENT

Figure 1 shows the experimental setup of electret generator, which consists of patterned electrets, counter electrodes, alignment stages, and an electromagnetic shaker [7]. 15-μm-thick CYTOP film is used as the electret. Width of interdigitized electrodes and electrets is 300 μm. After corona charging, surface voltage of the electret is -545 V. Total area of the electret and the gap between electrets and counter electrodes are respectively 20 x 20 mm^2 and 70 μm. Oscillation frequency f is 20 Hz, and amplitude is changed between 0.6 and 1.2 mm_{p-p}. Figure 2 shows output power versus purely-resistive external load. The peak power is proportional to the amplitude, which is in accordance with theoretical power output of the capacitor model [3, 4]. For 1.2 mm_{p-p} oscillation, maximum output of 13.7 μW is obtained with an external load of 13 MΩ.

Since output impedance of the electret generator is in MΩ range, impedance conversion as well as rectification is necessary to drive actual electronic circuits. Figure 2 shows the present power management circuit including a rectifier, a storage capacitor, and an autonomous analogue switch using transistors [8]. Charges are stored in the capacitor until the voltage reaches its threshold, and intermittently delivered to a LED. The present circuit requires no external power for wake-up, and consumes only 80 nA. Using this impedance conversion circuit, we demonstrate that a LED can be operated intermittently [8].

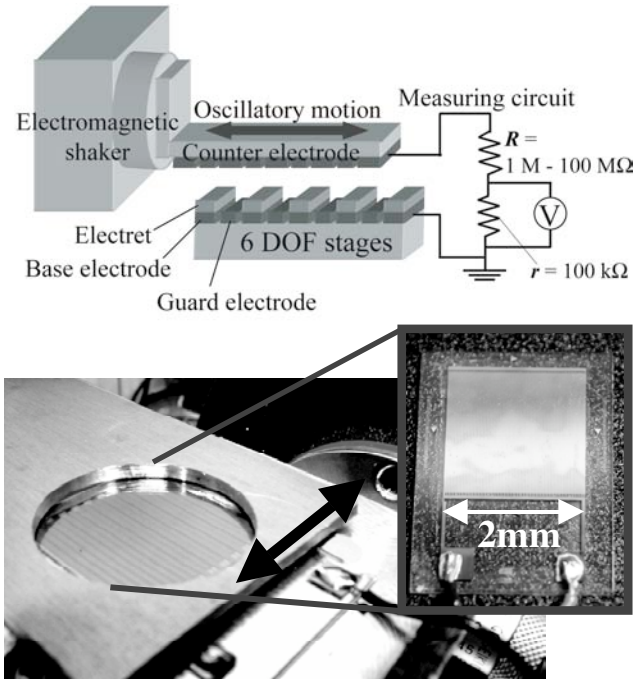

Figure 1. Setup for power generation experiment with forced oscillation.

NUMERICAL MODEL OF THE GENERATOR

Figure 4 shows a generator model with the power management circuit, where σ, d, and g are respectively the surface charge density, the thickness of electret film, the gap between the electret and the counter electrode.

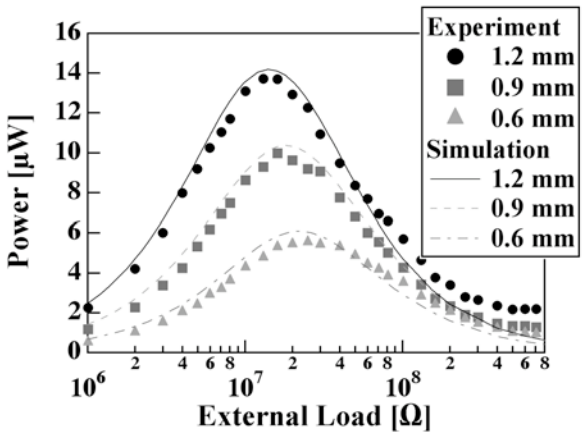

Figure 2. Power output versus external load at f =20 Hz.

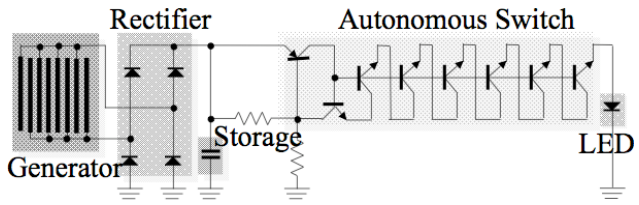

Figure 3. Low-power-consumption power managing circuit for rectifying and impedance conversion [8].

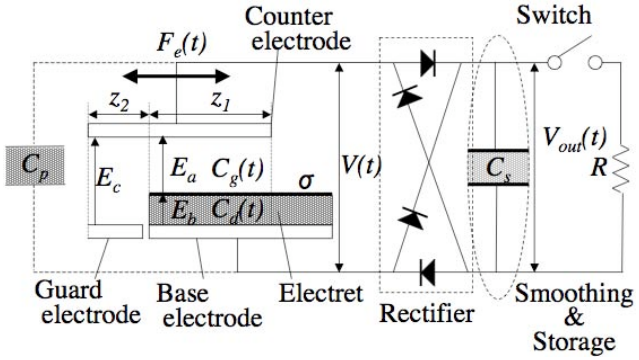

Figure 4. Computational model of electret generator with the power managing circuit.

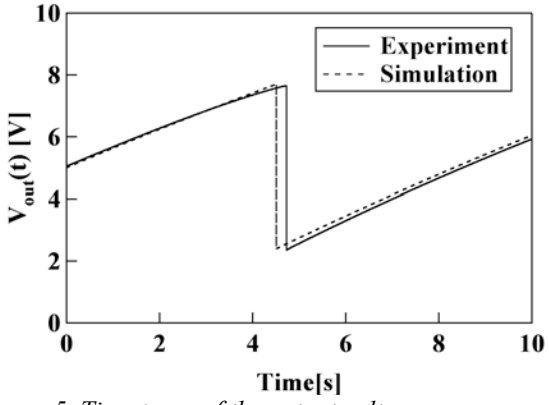

Figure 5. Time trace of the output voltage.

One-dimensional electrostatic field is assumed in this model. A differential equation based on Gauss' and Kirchhoff's laws as well as charge conservation is given by Eq. (1) and solved numerically [11], i.e.,

$$\frac{d}{dt}\left(\sigma_{i1} b z_1 + \sigma_{i2} b z_2\right) + C_p \frac{dV}{dt} + C_s \frac{dV_{out}}{dt} + \frac{V_{out}}{R} = 0 , \qquad (1)$$

where σ_{i1} and σ_{i2} are induced charge densities on the counter electrode facing respectively to the electret and the guard electrode as shown in Fig. 4. The quantity b represents length of the electrodes. C_p and C_s are respectively the parasitic capacitance between adjacent electrodes and the storage capacitance (C_s=1 μF).

In the present simulation, a full wave rectify circuit is assumed, and $V=V_{out}$ or $V=-V_{out}$ depending on the direction of current. Forward-voltage drop of each diode is set to 1.5 V. The autonomous analogue switch for intermittent discharge is designed to close and open respectively at 7.75 V and 2.35 V. Note that we neglect other unwanted characteristic of circuits such as leakage current and parasitic capacitance of the circuit.

By solving Eq. (1), we can get the output voltage V_{out}. The electrostatic damping force acting on the seismic mass is obtained with the energy conservation equation given by

$$\frac{dE_s}{dt} + \frac{d}{dt}\left(\frac{1}{2} C_p V^2 + \frac{1}{2} C_s V_{out}^2\right) + \frac{V_{out}^2}{R} + F_e \frac{dz}{dt} = 0 , \qquad (2)$$

where E_s, F_e, and z are respectively the electrostatic potential, the electrostatic force in the horizontal direction, and the displacement of the seismic mass. In the present simulation, the two-phase electrode arrangement is adopted [10, 11] in order to reduce unidirectional damping force.

In order to couple Eq. (1) with the motion of the seismic mass, we simultaneously solve the equation of motion under external vibration

$$m\ddot{z} + D_m \dot{z} + kz - F_e = -m\omega^2 y_0 \sin \omega t , \qquad (3)$$

where m, D_m, k, y_0, and ω are respectively mass of the seismic mass, parasitic damping coefficient of the spring system, the spring constant, the external vibration amplitude, and its angular frequency.

SIMULATION RESULTS

Firstly, simulation for purely-resistive load is made with the same parameters as in the experiment. The parasitic capacitance is chosen as C_p= 110 pF. As shown in Fig. 2, the numerical results for different amplitudes are in good agreement with the present experimental data. In addition, voltage signal obtained is also in accordance with the experimental data (not shown). Therefore, we confirm that the present model is sufficiently accurate to mimic the response of the generators.

Figure 5 shows a time trace of the output voltage with the power management circuit. Oscillation frequency and amplitude are respectively 10 Hz and 1.2 $mm_{p\text{-}p}$. In the present experiment, the discharge switch autonomously

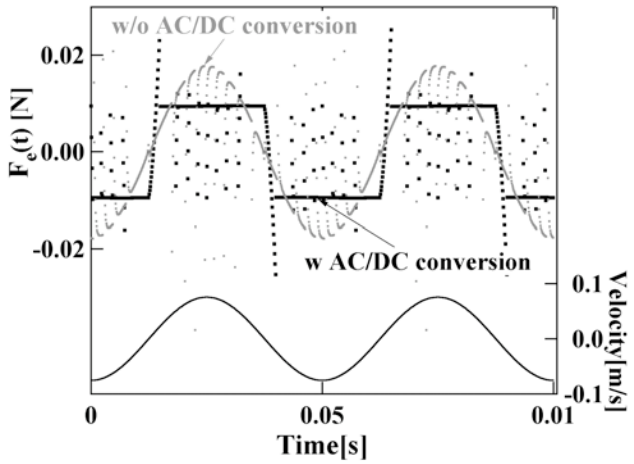

Figure 6. Electrostatic damping force in the horizontal direction.

Table 1: Parameters of the coupled simulation after [8].

Electrode length: b	14.6 mm
Width of electret: w	150 μm
Thickness of electret: d	15 μm
Width of seismic mass: W	16 mm
Seismic mass: m	1 g
Quality factor: Q	7.8
Surface voltage: V_s	-600 V
Parasitic capacitance: C_p	30 pF
Oscillation frequency: f	20 Hz
Maximum traveling length: z_{lim}	1 mm

close with an interval of 9.0 s, and 27.3 μJ is delivered to the LED in 1.4 ms, which corresponds to 29.4 % of the impedance-matched power output for purely-resistive load of 3 MΩ. Since the simulation result, in which no electrical loss is taken into account, is in agreement with the experimental data, the lower power output with the present power management circuit is due to the generator operation out of the impedance-matched point.

Figure 6 shows the electrostatic damping force acting on the seismic mass. When the external circuit is purely resistive, the electrostatic force becomes sinusoidal, which is close to the velocity-damped resonant generator (VDRG) [13]. On the other hand, when the present power management circuit is assumed, the electrostatic force becomes a square wave, which is similar with the coulomb-damped resonant generator (CDRG) [13]. Therefore, the external circuit has a large effect not only on the power output but also the damping force.

In the following sections, results for electromechanical coupled simulation are shown. The parameters are based on the electret generator prototype of Edamoto et al. [8] and summarized in Table 1. Figure 7 shows motion of the seismic mass $z(t)$, output voltage $V_{out}(t)$, and electrostatic damping force $F_e(t)$. When y_0=130 μm and g=20 μm (Fig. 7a), F_e is increased continuously with V_{out} during charging the capacitor, and thus the amplitude of $z(t)$ is gradually decreased due to larger damping force. When the switch is

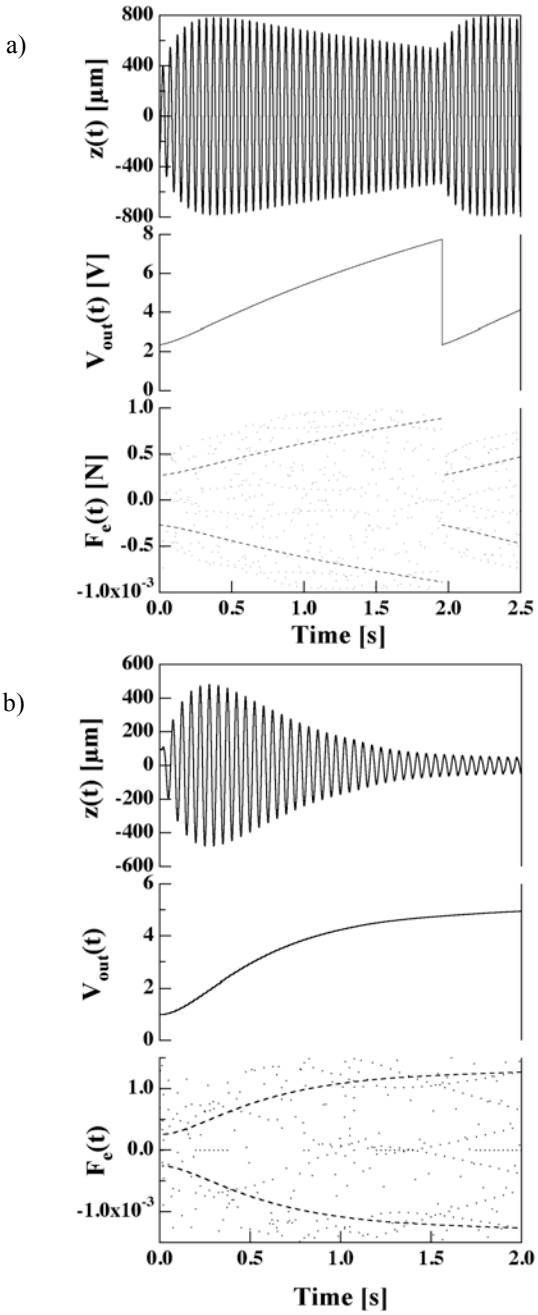

Figure 7. Time trace of motion of the seismic mass $z(t)$, output voltage $V_{out}(t)$, and electrostatic damping force $F_e(t)$. a) g=20 μm and y_0=130 μm, b) g=5 μm and y_0=100 μm.

closed, V_{out} is dropped due to discharge. Then, the amplitude suddenly goes back in response to reduction of the damping force. Therefore, mean amplitude of $z(t)$ within z_{lim} and thus the power output should become smaller than those for purely-resistive load.

On the other hand, when y_0=100 μm and g=5 μm, i.e., with smaller inertia force and larger damping force, F_e becomes large, so that the amplitude of $z(t)$ is almost damped out as shown in Fig. 7b. Thus, V_{out} becomes leveled-off, and doesn't reach the threshold voltage for discharge. Therefore, with the nonlinear power management circuit, there exists minimum y_0, under which

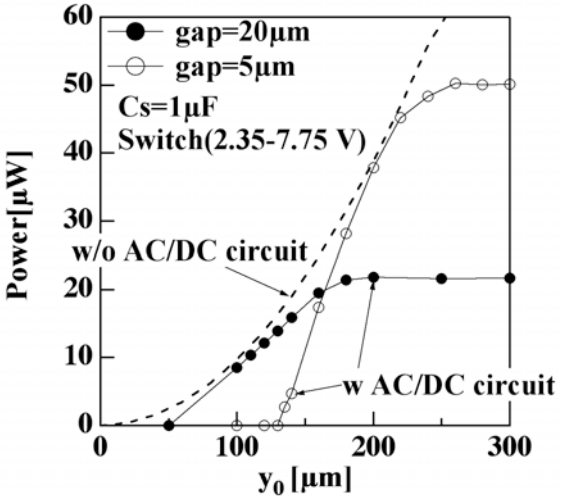

Figure 8. Output power versus external oscillation amplitude y_0.

no power is available due to overdamping.

Figure 8 shows the power output versus y_0 for two specific generator designs with different gap. Power output for the impedance-matched purely-resistive circuit is also plotted, which is proportional to y_0^2. When g=5 μm, the power output becomes zero for y_0<140 μm, while it levels off at y_0>250 μm. Thus, the generator with this design is only efficient in the external amplitude range of about 150<y_0<250 μm. On the other hand, when g=20 μm, power output is available for y_0 down to about y_0=60 μm. However, because of its smaller damping factor, the maximum power output with the limited traveling distance z_{lim} becomes much smaller. These results demonstrate that optimum design of the generator is necessary under given operation condition.

CONCLUSION

We develop a complete numerical model of the vibration-driven micro electret power generator with nonlinear power management circuit, and investigate its effect on the electro-mechanical performance of the generators. The following conclusions can be derived:

- The electromechanical model can properly mimic response of the generators in the present experiments.
- The electrostatic damping force is strongly dependent on nonlinearity of the external circuit.
- Impedance conversion with switching could cause intermittent excess amplitude for large external vibration and/or overdamping for low external vibration, in which the conversion efficiency of generators is deteriorated.
- With a nonlinear external circuit, optimum design of the generator is necessary under given operation condition.

This work is partially supported by the New Energy and Industrial Technology Development Organization (NEDO) and the Ministry of Internal Affairs and Communications (MIC) of Japan.

REFERENCES

[1] J. A. Paradiso, and T. Starner, "Energy scavenging for mobile and wireless electronics," IEEE Pervasive Comp., Vol. 4, pp. 18-27, 2005.

[2] S. P. Beeby, M. J. Tudor, and N. M. White, "Energy harvesting vibration sources for micro systems applications," Meas. Sci. Technol., Vol. 17, pp.175-195, 2006.

[3] J. Borland, Y.-H. Chao, Y. Suzuki, and Y.-C. Tai, "Micro electret power generator," Proc. 16th IEEE Int. Conf. MEMS, Kyoto, pp. 538-541, 2003.

[4] T. Tsutsumino, Y. Suzuki, N. Kasagi, and Y. Sakane, "Seismic power generator using high-performance polymer electret," Proc. 19th IEEE Int. Conf. MEMS, Istanbul, pp. 98-101, 2006.

[5] Y. Naruse, N. Matsubara, K. Mabuchi, M. Izumi, and K. Honma, "Electrostatic micro power generator from low frequency vibration such as human motion," Proc. PowerMEMS 2008, Sendai, pp. 19-22, 2008.

[6] H.-W. Lo, and Y.-C. Tai, "Parylene-based electret power generators," J. Micromech. Microeng., Vol. 18, 104006, 8pp, 2008.

[7] Y. Sakane, Y. Suzuki, and N. Kasagi, "Development of high-performance perfuluoriented polymer electret film and its application to micro power generation," J. Micromech. Microeng., Vol. 18, 104011, 6pp, 2008.

[8] M. Edamoto, Y. Suzuki, N. Kasagi, K. Kashiwagi, Y. Moizawa, T. Yokoyma, T. Seki, and M. Oba, "Low-resonant-frequency micro electret generator for energy harvesting application", Proc. 22nd IEEE Int. Conf. MEMS, Sorrento, pp. 1059-1062, 2009.

[9] Y. Suzuki, and Y.-C. Tai, "Micromachined high-aspect-ratio parylene spring and its application to low-frequency accelerometers," J. Microelectromech. Syst., Vol. 15, pp.1364-1370, 2006.

[10] T. Tsutsumino, Y. Suzuki, N. Kasagi, "Electro-mechanical modeling of micro electret generator for energy harvesting", Proc. Transducers '07, Lyon, Vol. 2, pp. 863-866, 2007.

[11] C. Marboutin, Y. Suzuki, and N. Kasagi, "Optimal design of micro electret generator for energy harvesting", Proc. PowerMEMS 2007, Freiburg, pp. 141-144, 2007.

[12] Y. Tada, "Experimental characteristics of electret generator using polymer film electrets," Jpn. J. Appl. Phys., Vol. 31, pp. 846–851, 1992.

[13] P. D. Micheson, T. C. Green, E. M. Yeatman, and A. S. Holmes, "Architectures for vibration-driven micropower generators," J. Microelectromech. Syst., Vol. 13, pp. 429-440, 2004.

CONTACT

Prof. Yuji Suzuki, Dept. of Mechanical Engineering, The University of Tokyo, ysuzuki@thtlab.t.u-tokyo.ac.jp